Long and short time scales of Intraseasonal variability in South America

Mariano S. Alvarez

Departamento de Ciencias de la Atmósfera y los Océanos, Facultad de Ciencias Exactas y Naturales, Universidad de Buenos Aires

Centro de Investigaciones del Mar y la Atmósfera (CIMA), UMI IFAECI/CNRS, CONICET/UBA

Buenos Aires, Argentina

The **objective** of this study is to determine patterns to describe the seasonal cycle of IS variability in SA and its relationship with both SH circulation anomalies and tropical convection.

The **final goal** is to create a frame for monitoring and predicting tools in the SESA region.

Methodology

- **Lanczos** filter with 101 weights to retain **10-30** and **30-90** days variability, applied to **OLR anomalies.**
- **EOF** using the covariance matrix of the IS-filtered OLR anomalies. Leading pattern retained, named Seasonal IntraSeasonal (**SIS**) **pattern**.
- Standardized PC1 (**SIS index**) as the time series to describe the activity of the SIS pattern.
- **Linear lagged regression maps** between PC1 and OLR anomalies and streamfunction anomalies at upper levels (0.21 sigma).
- **Wave activity fluxes** computed from the regression as a proxy for energy dispersion along the wave trains.

Rainy season: October to April

IS variability in 30-90 days

3090-SIS Pattern

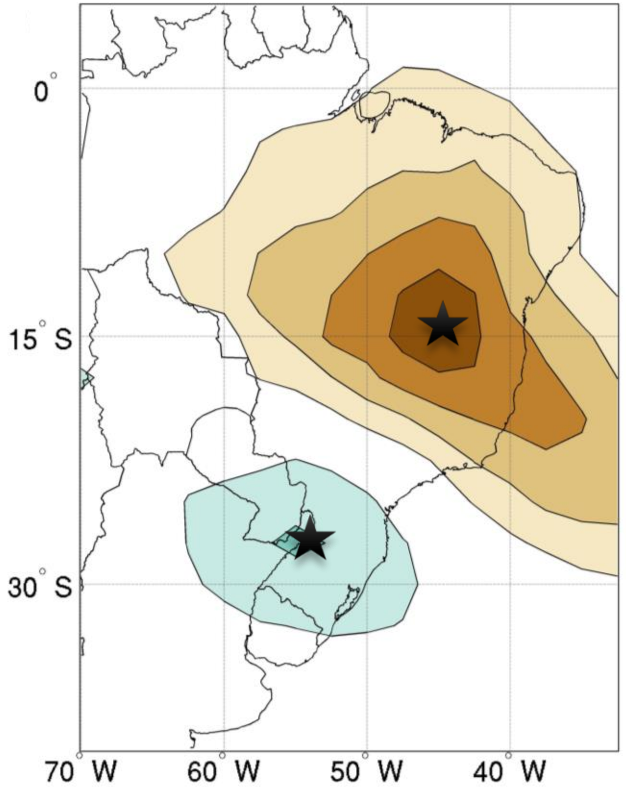

First EOF of FOLR 30-90 (21.5% of explained variance)

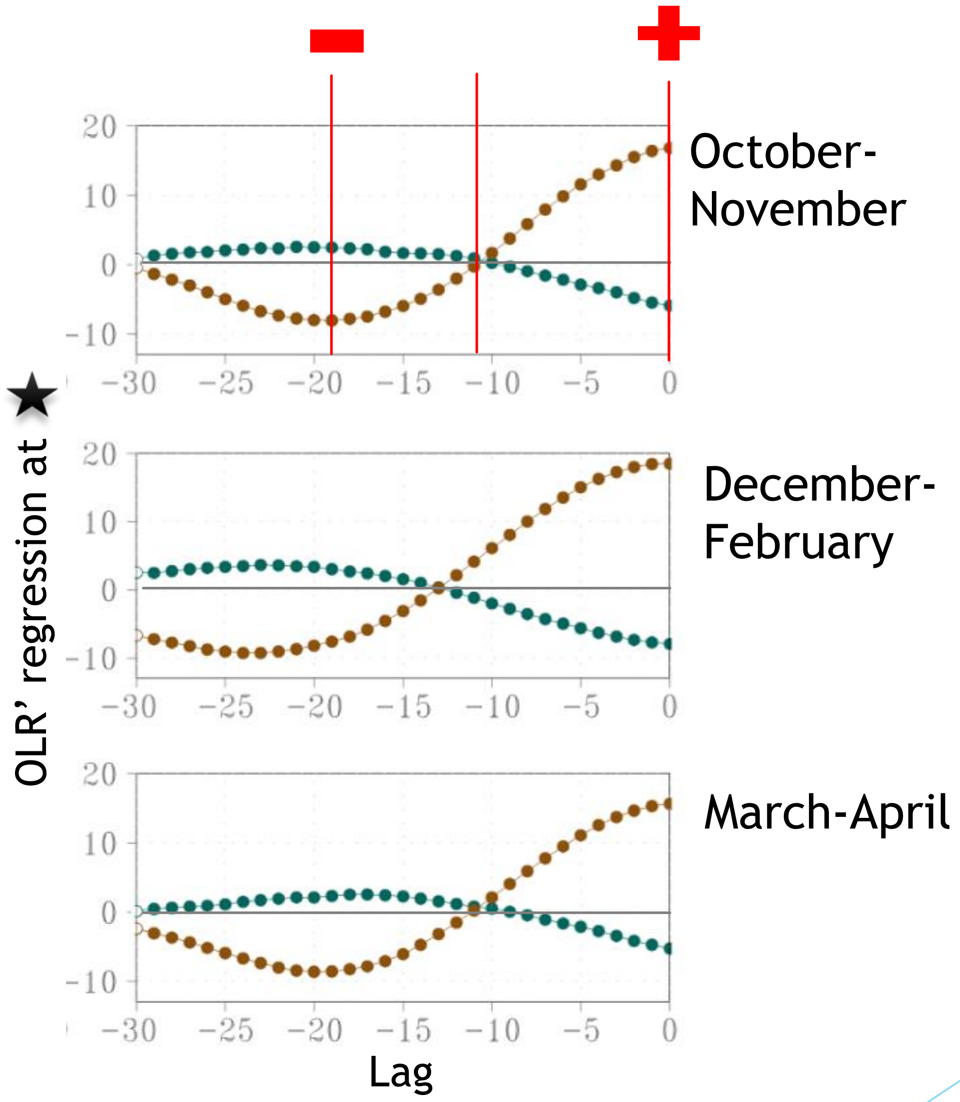

Rainy season: October to April

IS variability in 30-90 days

Lagged regression maps: PC1 and OLR anomalies

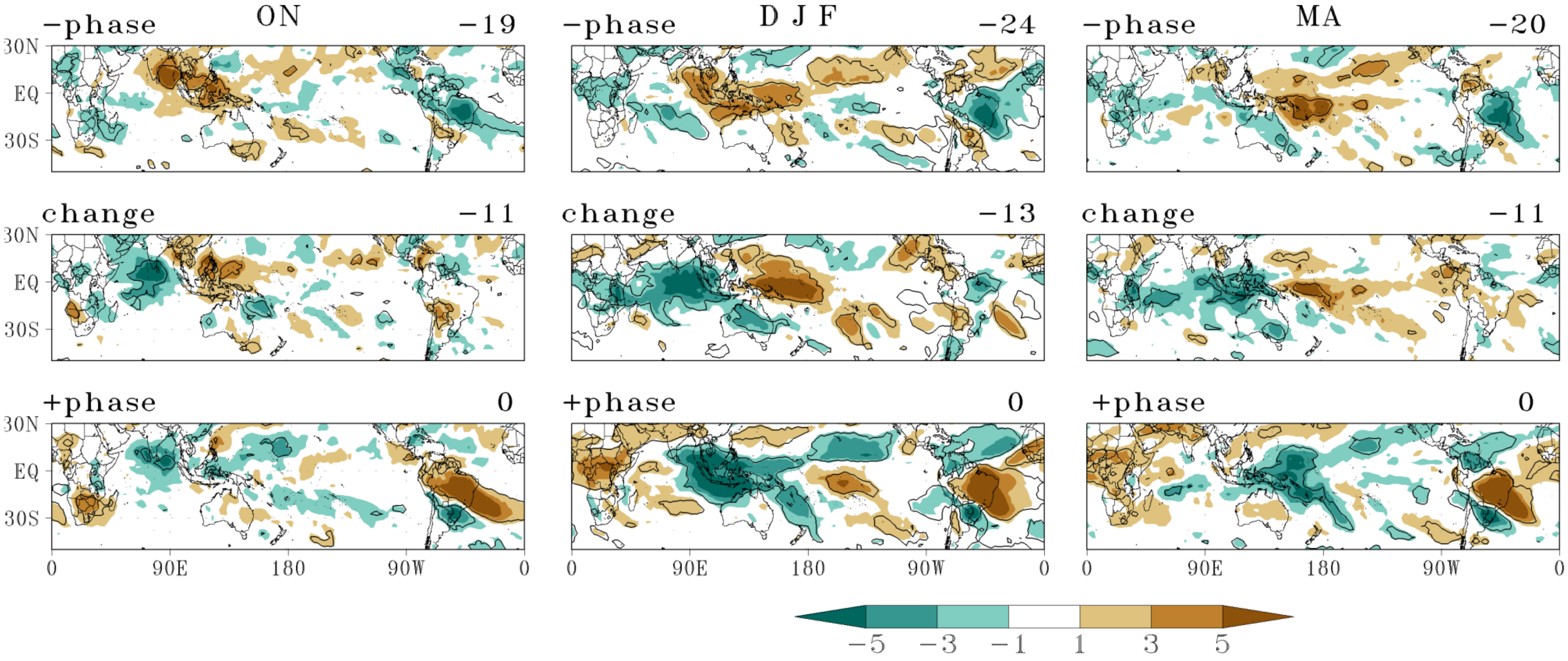

Maps of linear lagged regressions between OLR anomalies and the standardized PC1 30-90 for each season, for those lags in which the leading pattern of FOLR 30-90 showed the most intense negative phase, a change of phase and the most intense positive phase

Rainy season: October to April

IS variability in 30-90 days

Lagged regression maps: PC1 and OLR anomalies

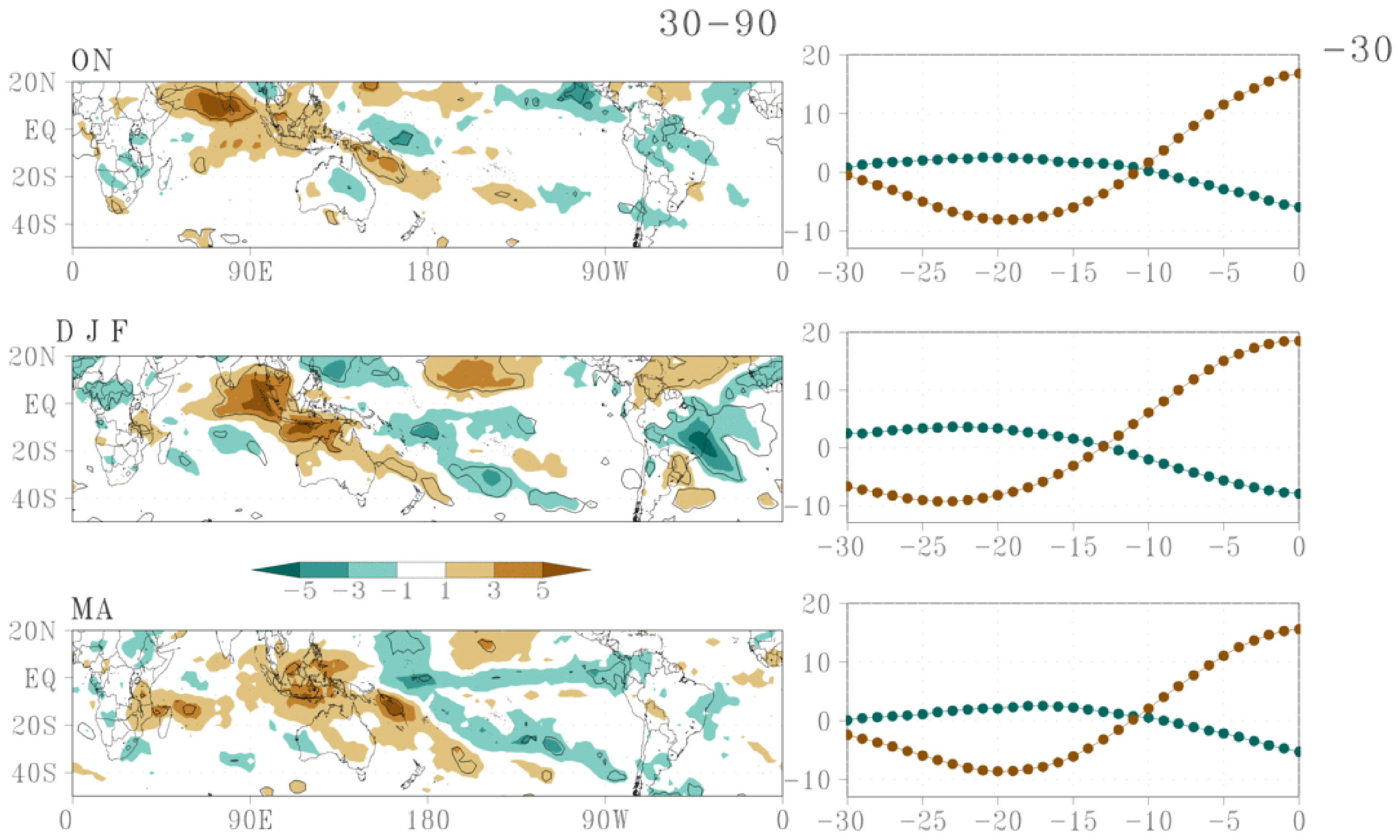

Maps of linear lagged regressions between OLR anomalies and the standardized PC1 30-90 for each season, for those lags in which the leading pattern of FOLR 30-90 showed the most intense negative phase, a change of phase and the most intense positive phase

Rainy season: October to April

IS variability in 30-90 days

Lagged regression maps: PC1 and 0.21-σ streamfunction anomalies

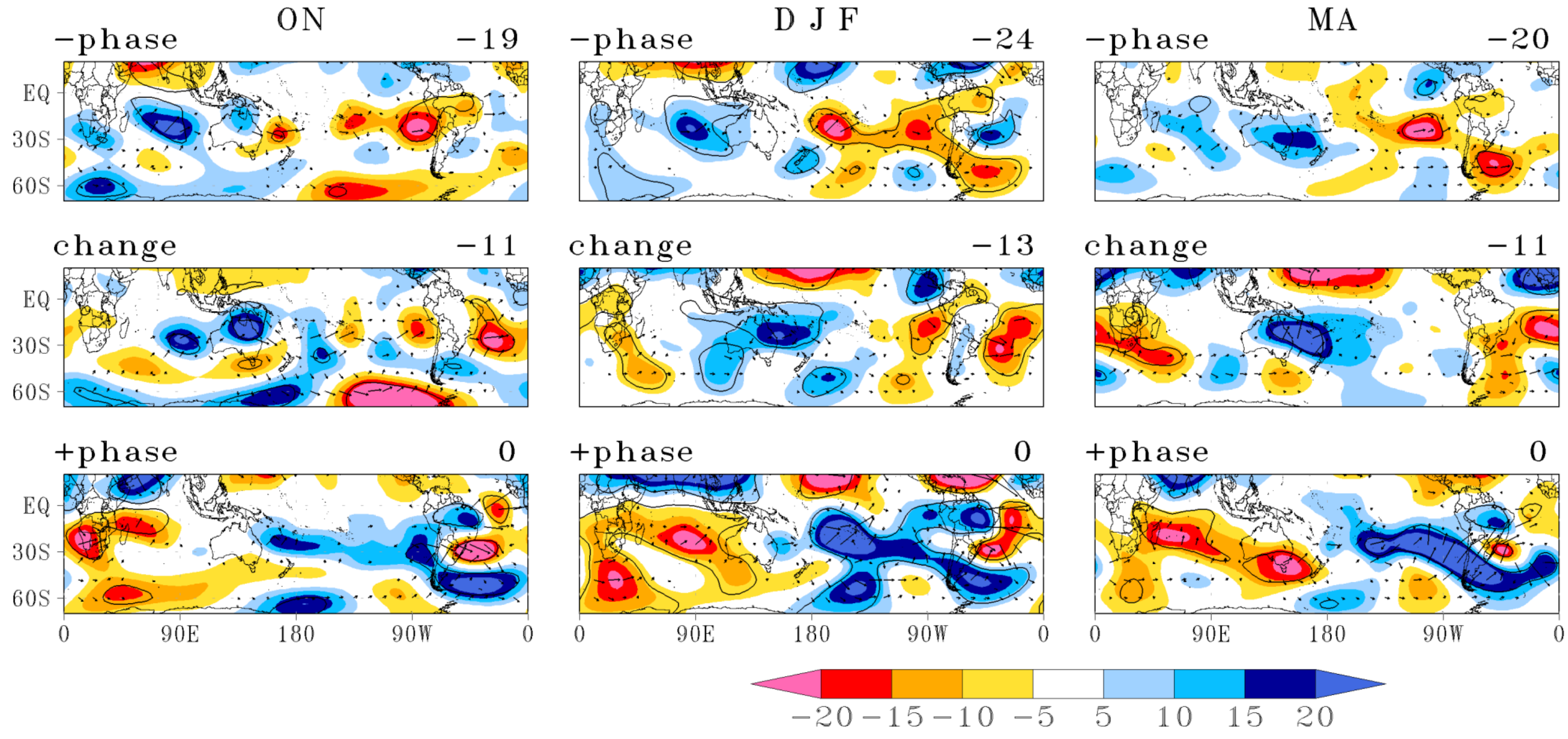

Maps of linear lagged regressions between 0.21 sigma-level streamfunction anomalies and the standardized PC1 30-90 for each season, for those lags in which the leading pattern of FOLR 30-90 showed the most intense negative phase, a change of phase and the most intense positive phase

Rainy season: October to April

IS variability in 30-90 days

Lagged regression maps: PC1 and 0.21-σ streamfunction anomalies

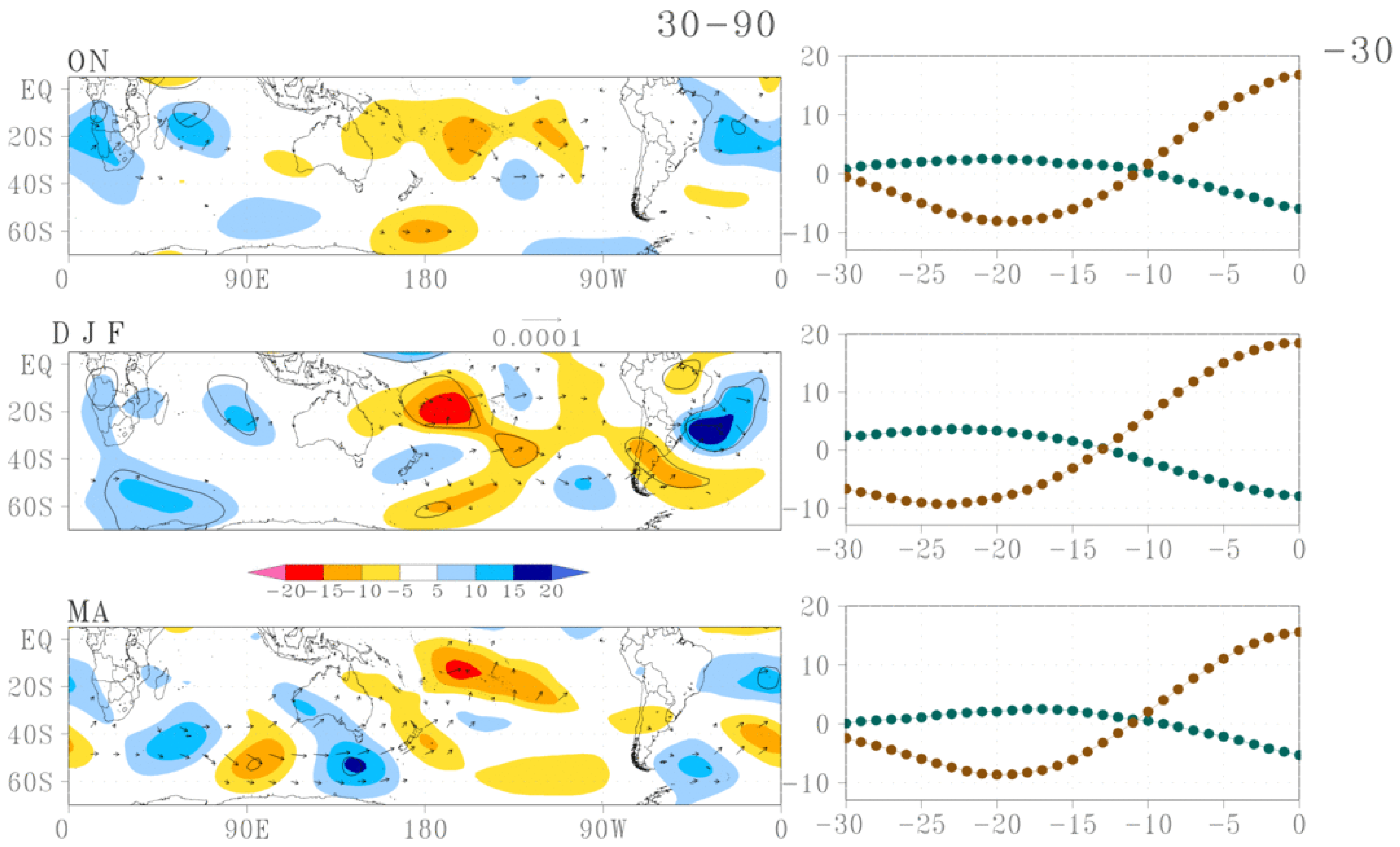

Maps of linear lagged regressions between 0.21 sigma-level streamfunction anomalies and the standardized PC1 30-90 for each season, for those lags in which the leading pattern of FOLR 30-90 showed the most intense negative phase, a change of phase and the most intense positive phase

Rainy season: October to April | IS variability in 30-90 days

Might the activity of the 3090-SIS pattern be related to the Madden-Julian Oscillation?

Previous work on MJO impacts on South American rainfall: Alvarez et al. 2016 (Clim. Dyn.)

Methodology

- **RMM index** used to characterize the MJO. Similar results found with OMI index (Kiladis et al. 2014).

- For each season (DJF, MAM, JJA, SON) the RMM index was related to rainfall following Wheeler et al. (2009), as **composites** of the probability of 7-day-running-mean rainfall of exceeding the upper tercile, expressed as a ratio respect to 0.33 (so 1 means nominal probability, 1.5 that 0.33*1.5=0.495 chance of exceeding the upper tercile, etc.)

Rainy season: October to April

IS variability in 30-90 days

DJF

MJO impacts in South America

DJF

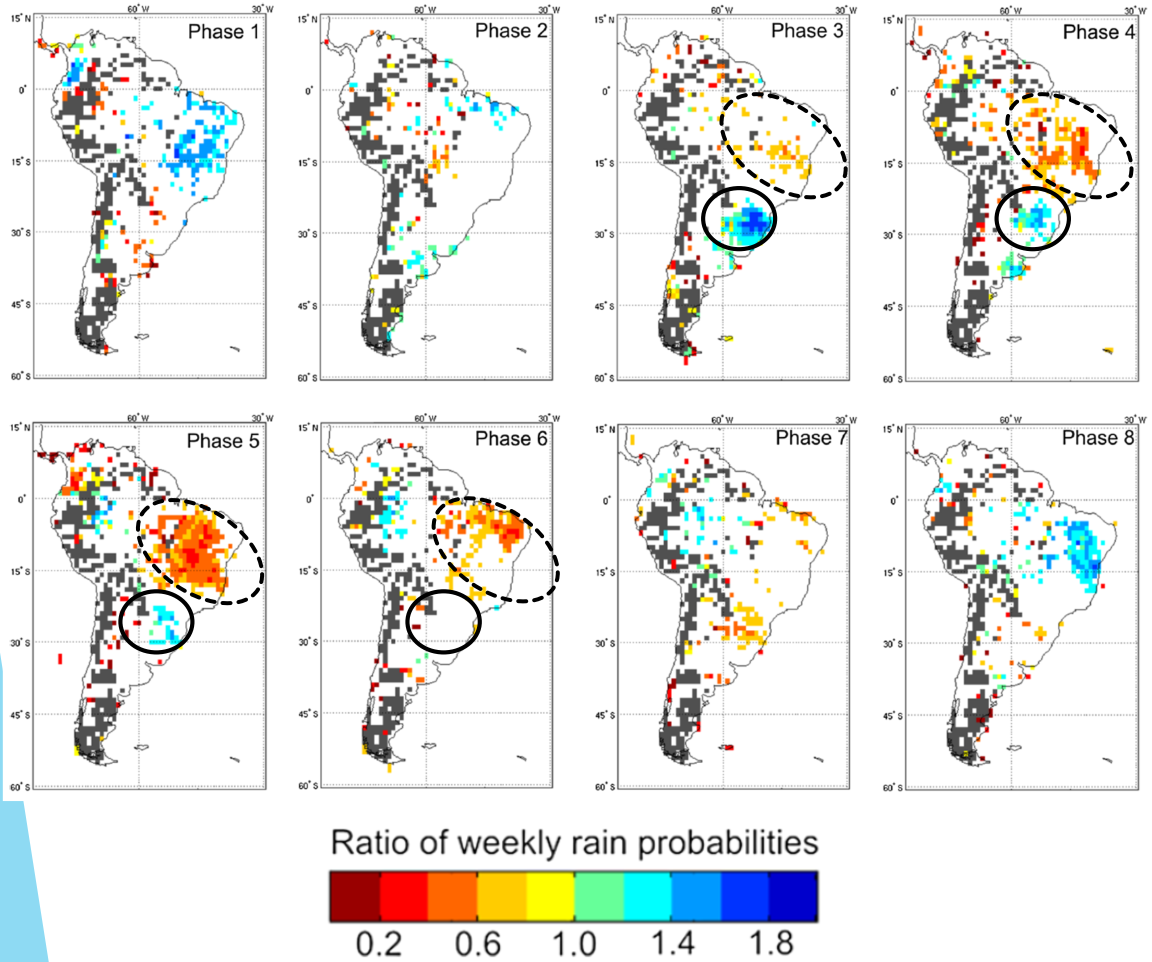

CHIRPS dataset using IRI data Library

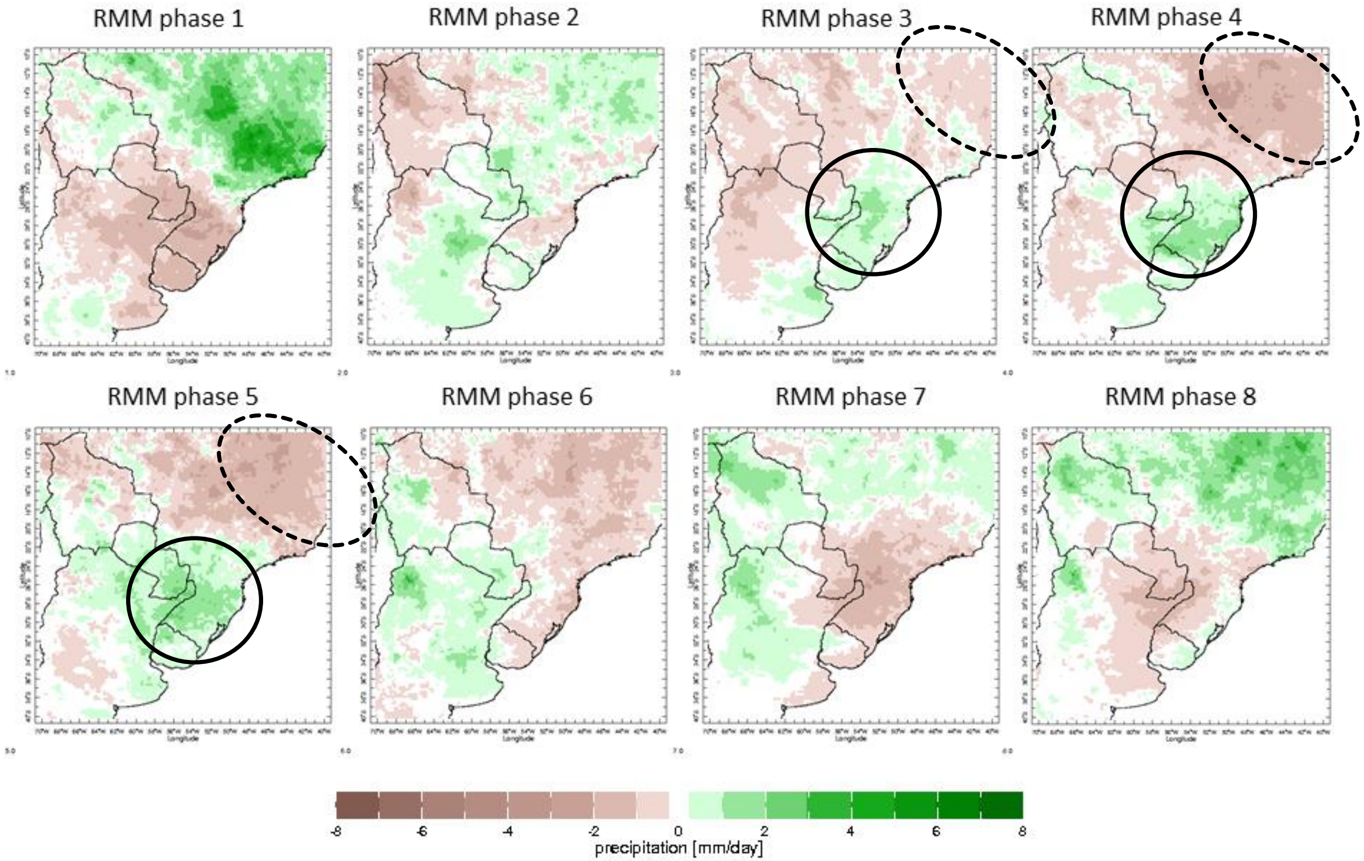

Rainy season: October to April

IS variability in 30-90 days

DJF

MJO impacts in South America

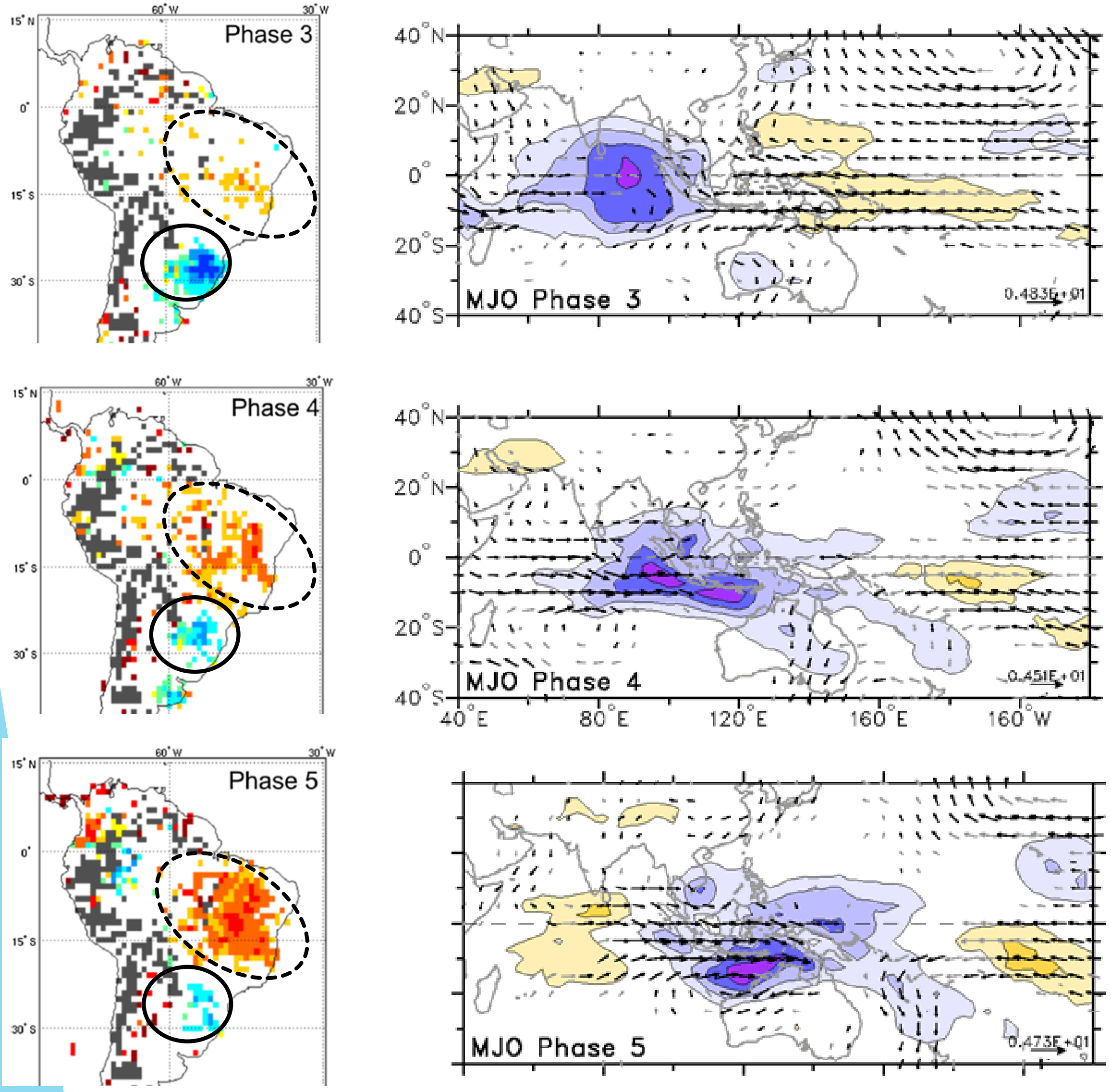

From BoM

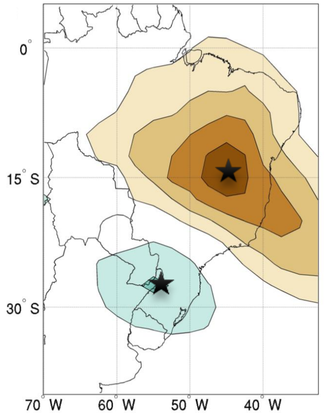

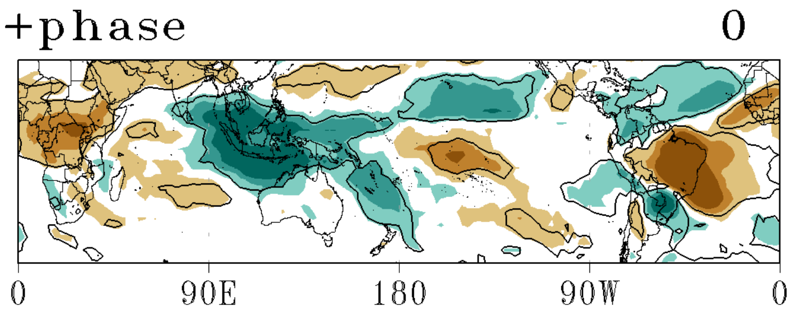

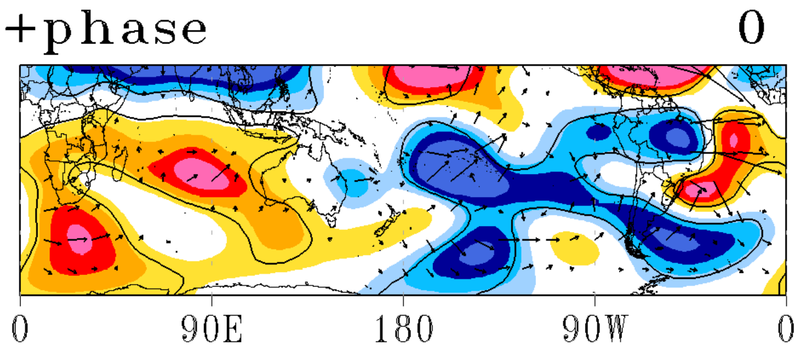

Rainy season: October to April | IS variability in 30-90 days

Is the activity of the 3090-SIS pattern related to the Madden-Julian Oscillation?

Methodology

- IS variability of the MJO activity described following Jones et al. (2012) and Matthews (2000). The **index** is computed as a **combined EOF using 200- and 850-hPa zonal wind** detrended anomalies, filtered with a Lanczos band-pass filter with cut-off periods of **20 and 200 days**.
  - Advantages respect to RMM index: less noisy, detects better isolated MJO events, captures IS variability of MJO
- The obtained PC1 and PC2 can be plotted, as RMM1 and RMM2, in a phase diagram.
- **MJO coherent events** defined if
  - (i) The amplitude of the MJO index is greater than 0.9 during the whole event
  - (ii) The MJO propagates eastwards (counter-clockwise rotation on phase diagram)
  - (iii) The event lasts more than 25 days.
- **3090-SIS index** positive (negative) **events**: at least 5 consecutive days greater (lower) than (-) 1

Rainy season: October to April

IS variability in 30-90 days

Relationship between SIS pattern activity and MJO

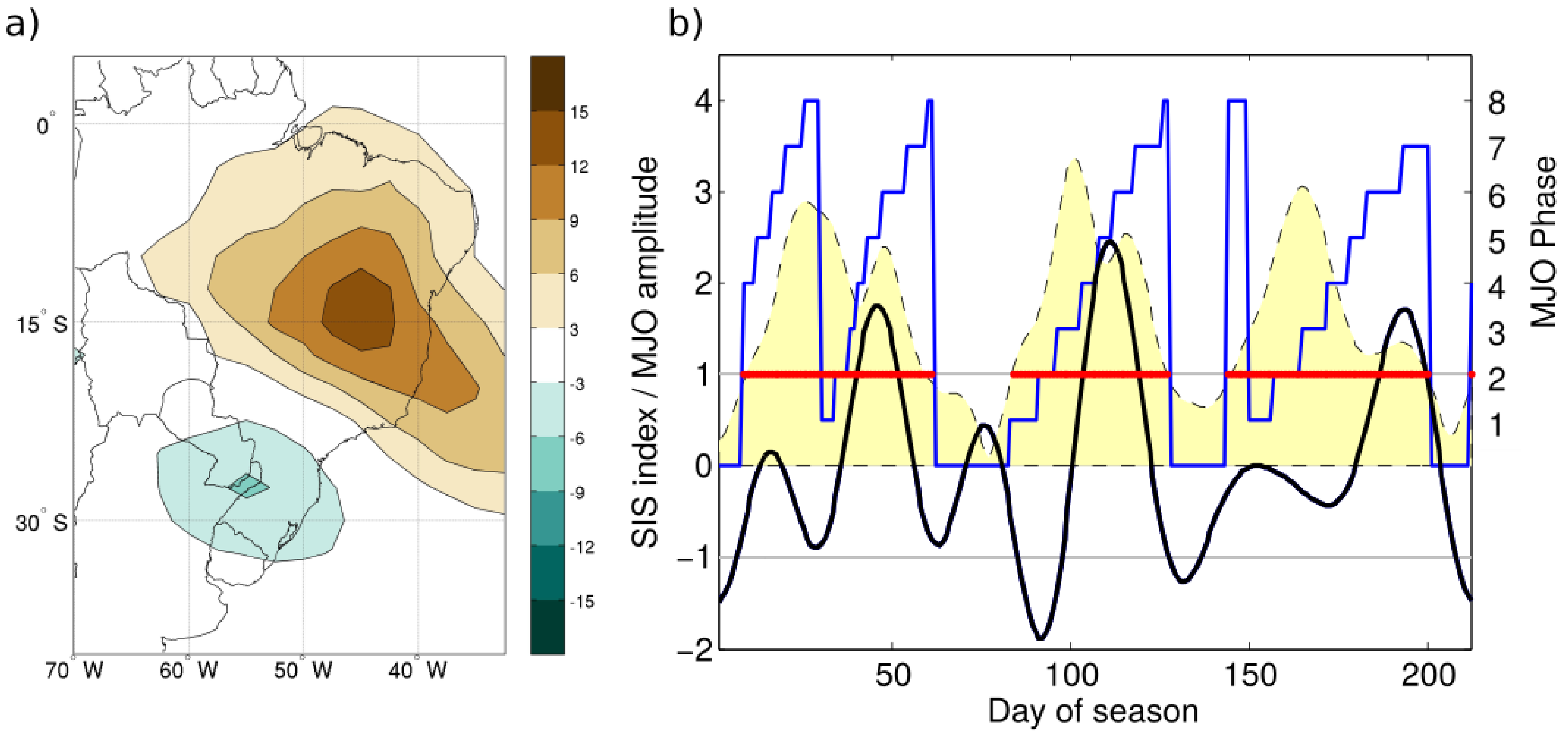

Positive SIS event: convection enhanced in SESA and suppressed in SACZ

3090-SIS index (PC1)

MJO amplitude ($\sqrt{PC1^2 + PC2^2}$)

MJO phase

MJO event

Rainy season: October to April

IS variability in 30-90 days

MJO index values for positive and negative SIS events

Positive SIS events

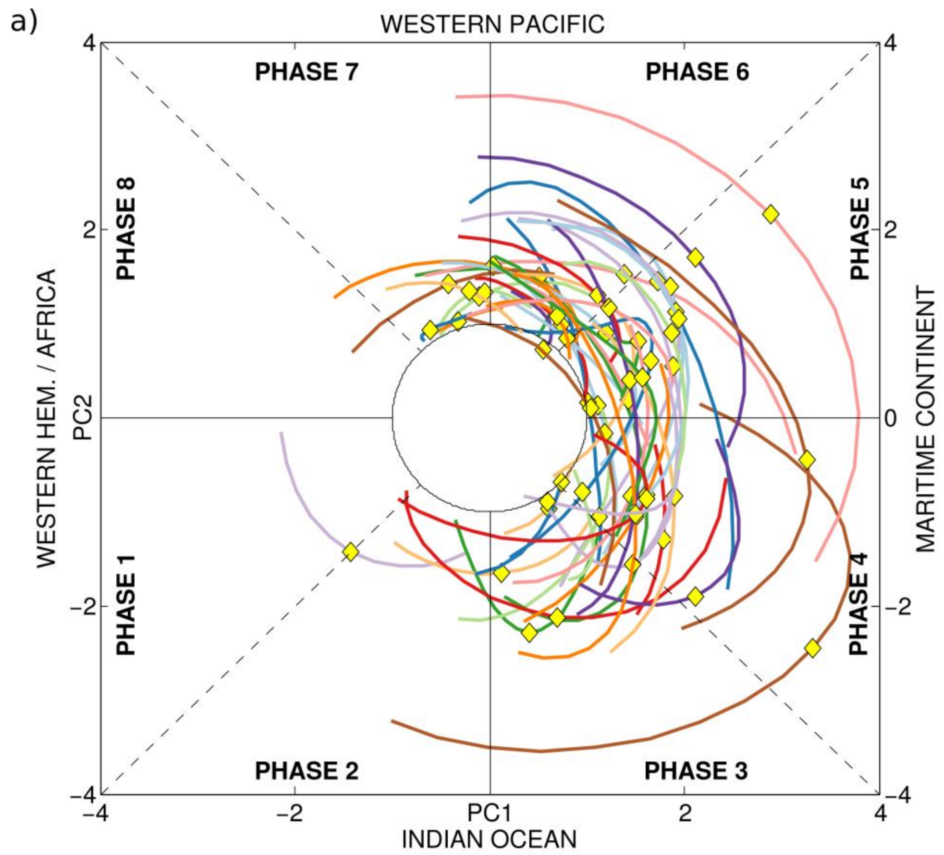

Negative SIS events

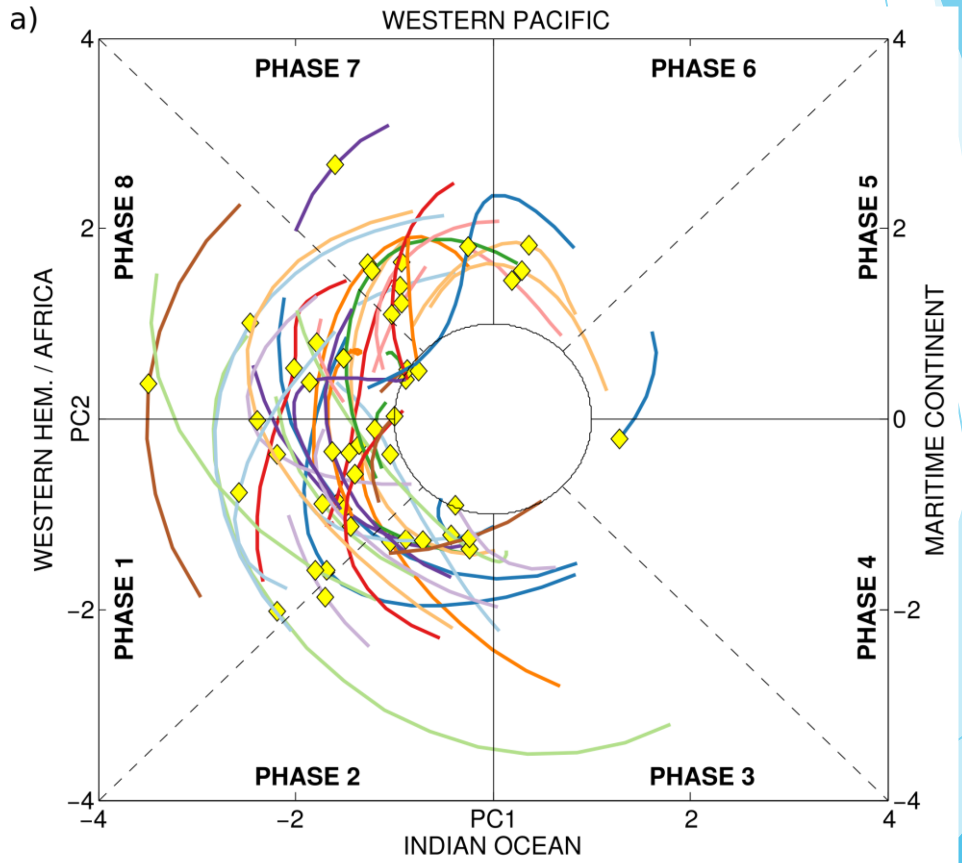

MJO phase diagram with the daily MJO index values during positive SIS events within an MJO event. The yellow diamond indicates the day in which the SIS index is maximum

Rainy season: October to April

IS variability in 30-90 days

MJO index values for positive and negative SIS events

Positive SIS events

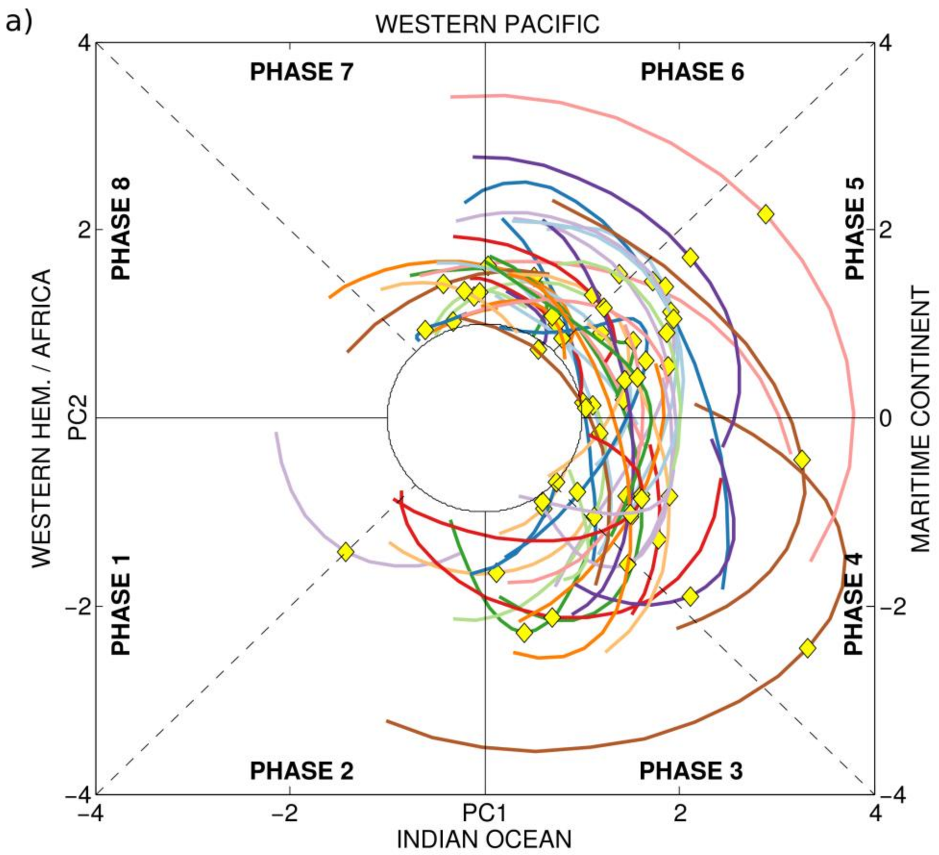

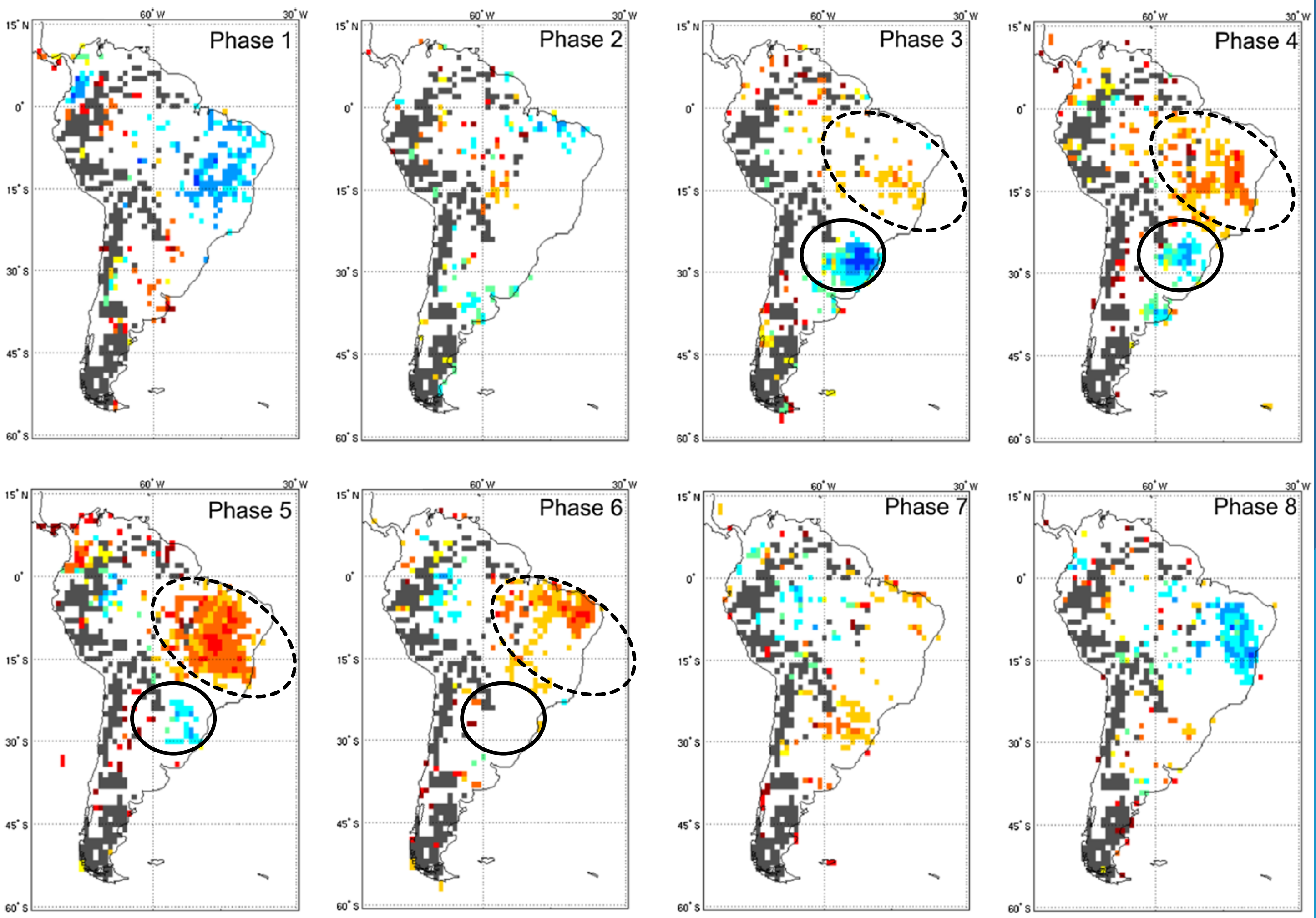

MJO phase diagram with the daily MJO index values during positive SIS events within an MJO event. The yellow diamond indicates the day in which the SIS index is maximum

Rainy season: October to April | IS variability in 30-90 days

MJO index values for positive and negative SIS events

Positive SIS events

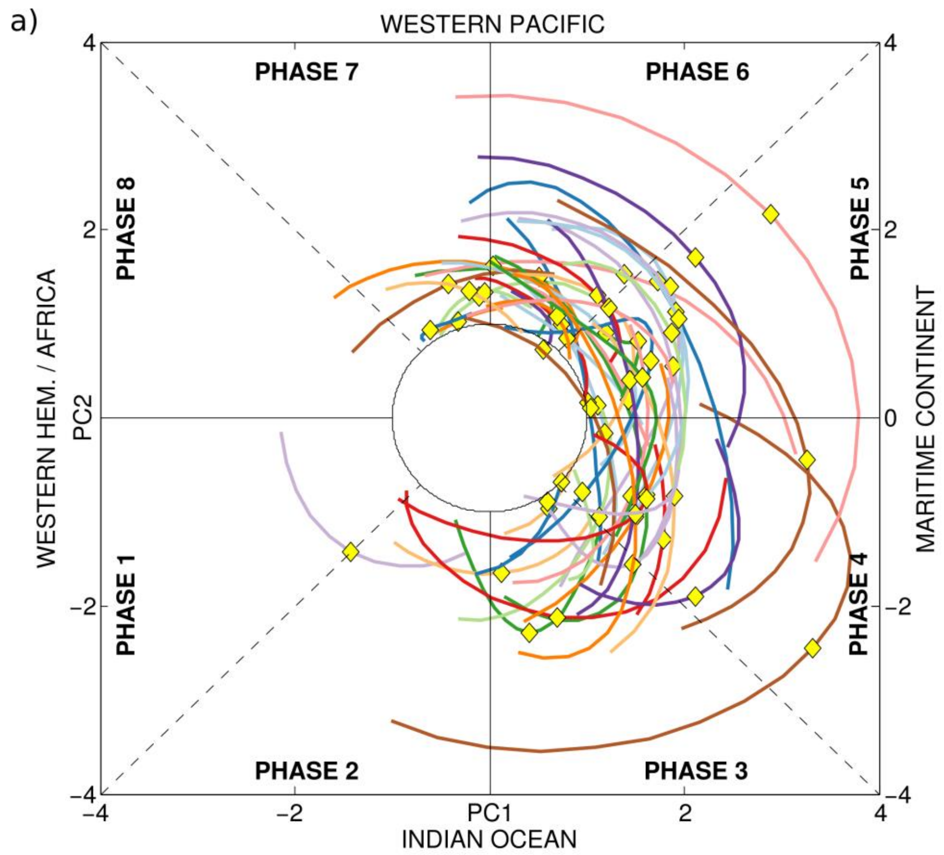

MJO phase diagram with the daily MJO index values during positive SIS events within an MJO event. The yellow diamond indicates the day in which the SIS index is maximum

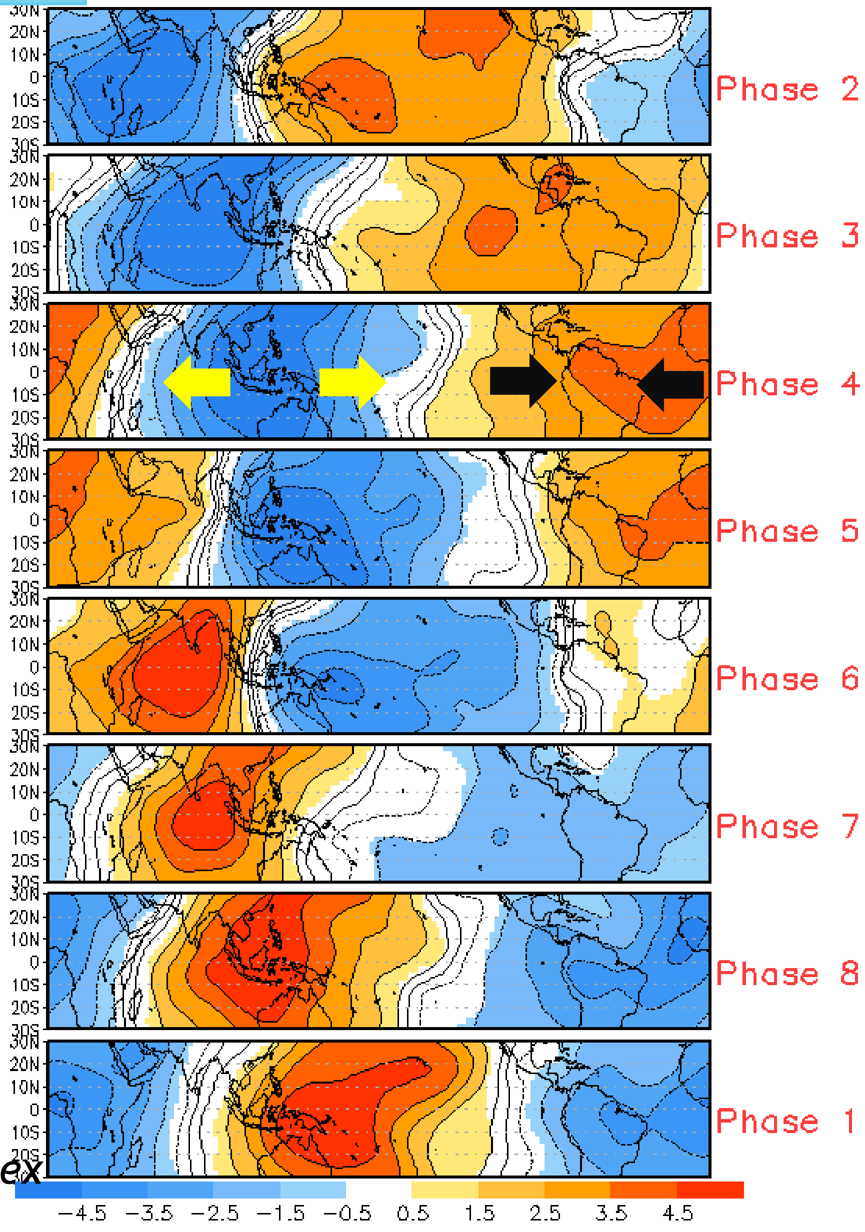

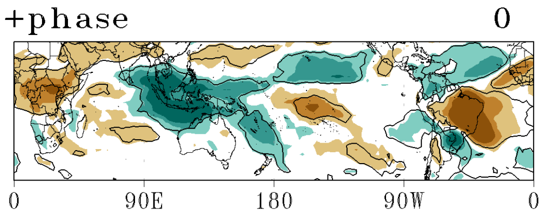

From CPC

Rainy season: October to April

IS variability in 30-90 days

MJO index values for positive and negative SIS events

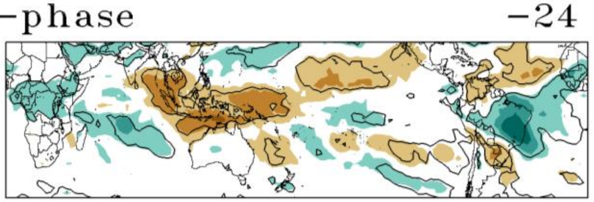

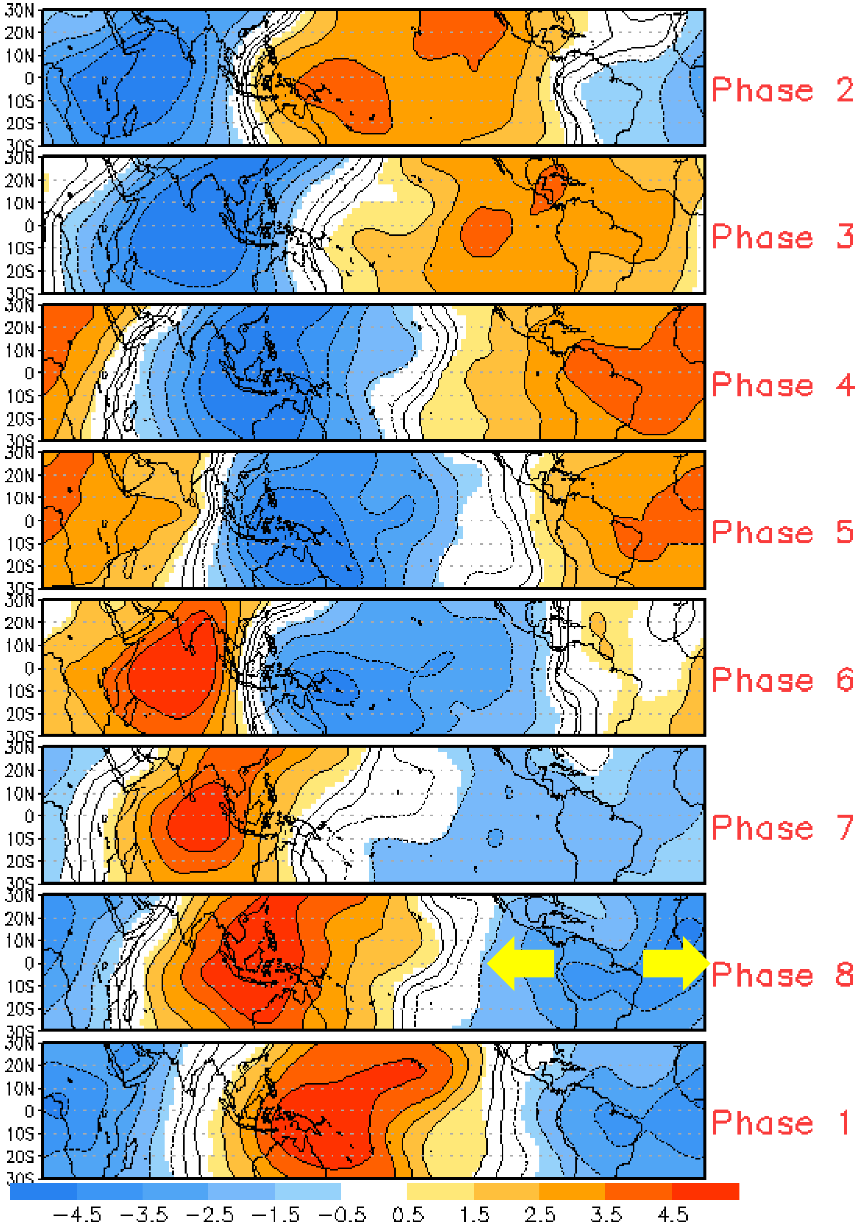

Negative SIS events

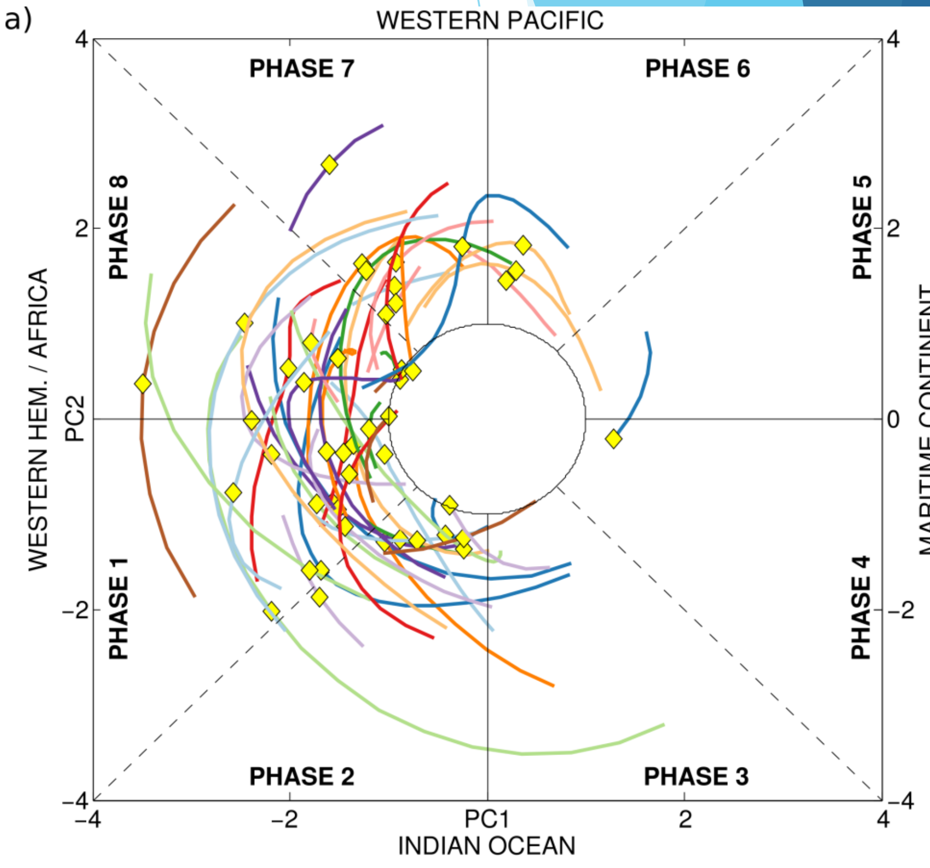

MJO phase diagram with the daily MJO index values during positive SIS events within an MJO event. The yellow diamond indicates the day in which the SIS index is maximum

Rainy season: October to April

IS variability in 30-90 days

3090-SIS index values for each MJO phase

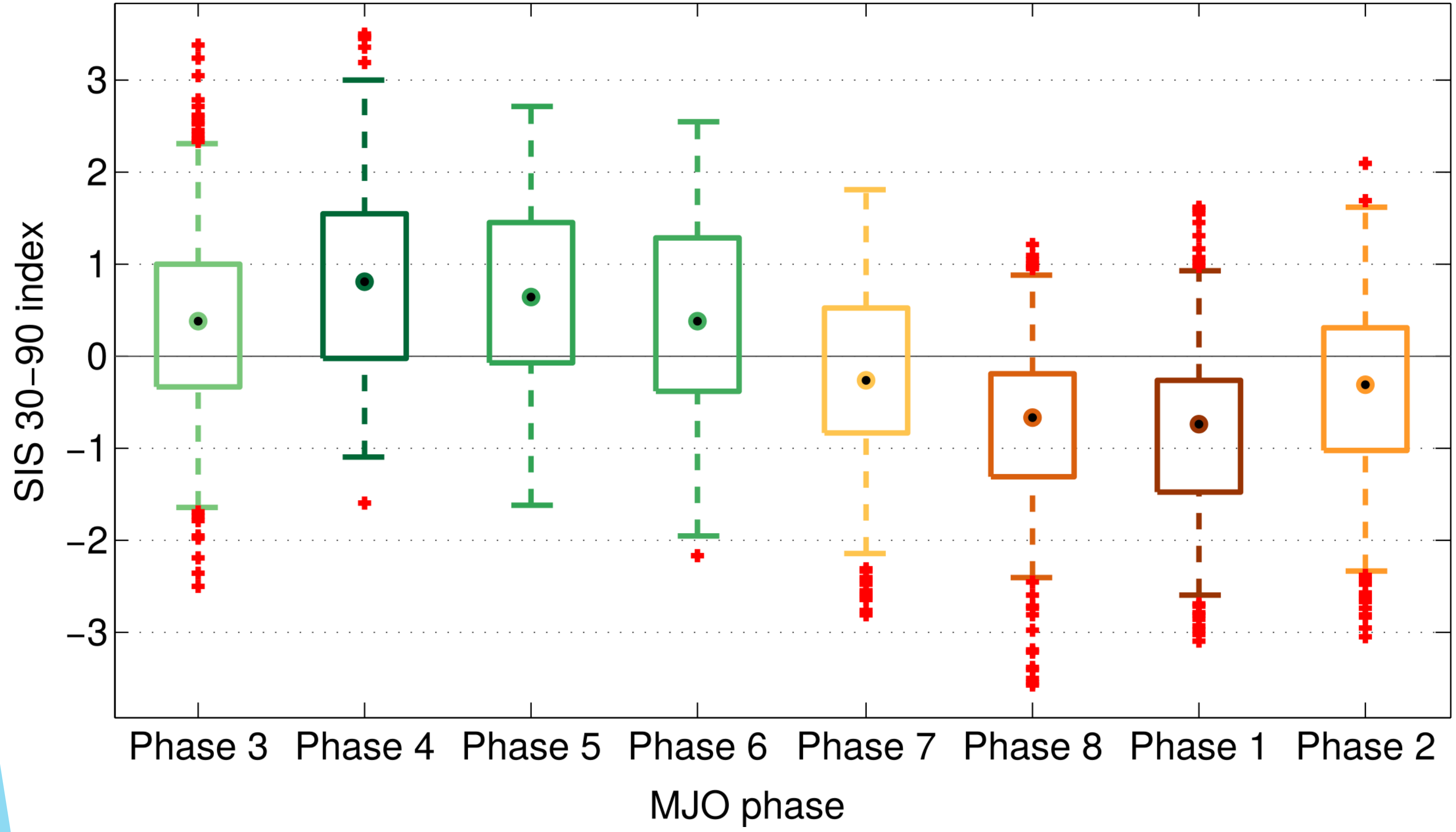

Box plot of the SIS index values for each MJO phase achieved within an MJO event

Rainy season: October to April | IS variability in 30-90 days

Highlights

- During the **rainy season**, the leading pattern of IS variability **(SIS pattern)** is a **dipole** with centers of action in the SACZ (more intense) and SESA (less intense) regions. Explained variability of: 21.5%

- PC1-based lagged regressions showed that the evolution towards a positive phase of the SIS pattern is **related to the progression of MJO-like tropical convection anomalies** to the east, with differences within the rainy season. Also, **extratropical wave trains** seem to link those convective anomalies to anomalies over South America.

- Previous studies regarding the MJO impacts in South America allowed to find similarities between the MJO progression and the evolution of the SIS patterns.

- **SIS positive events occur during MJO** phases 3,4,5,6, while negative SIS events are favored during MJO phases 7,8,1,2.

To address

- Disentangle the MJO signal on SIS events to analyze the phase in which the teleconnections that impact in SESA are first generated (precursors of SIS events).

- Use OMI to characterize MJO events and compare to these results.

Dry season: March to September | IS variability in 30-90 days

3090-SIS Pattern and linear lagged regressions of OLR anomalies and 0.21-σ streamfunction

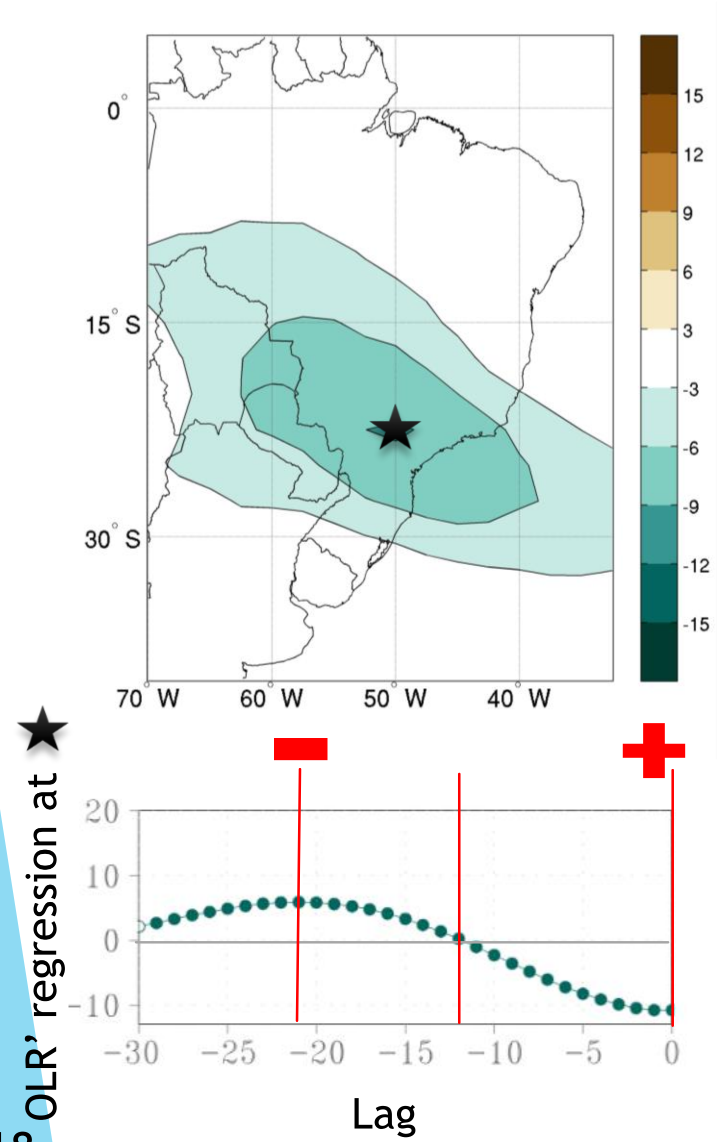

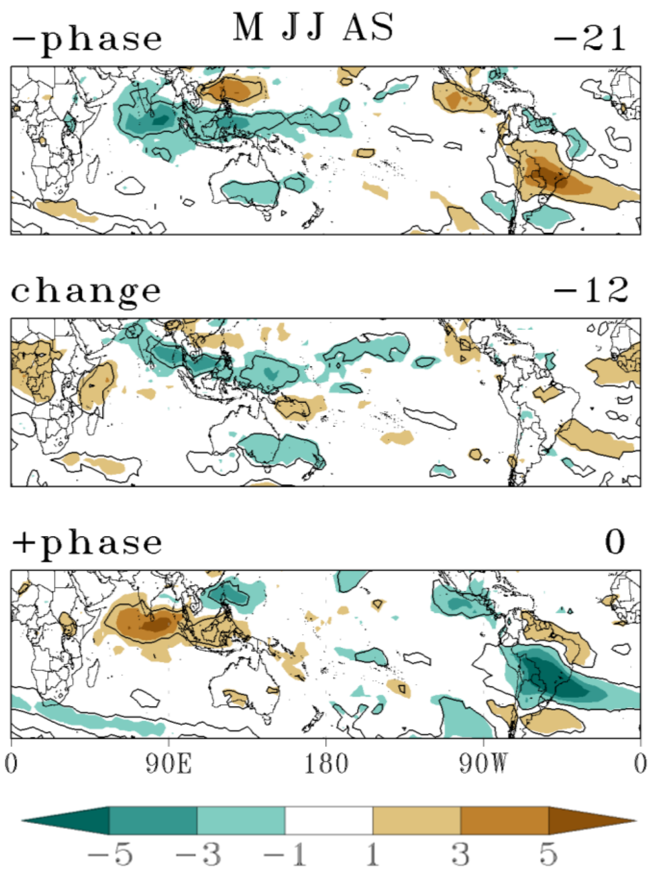

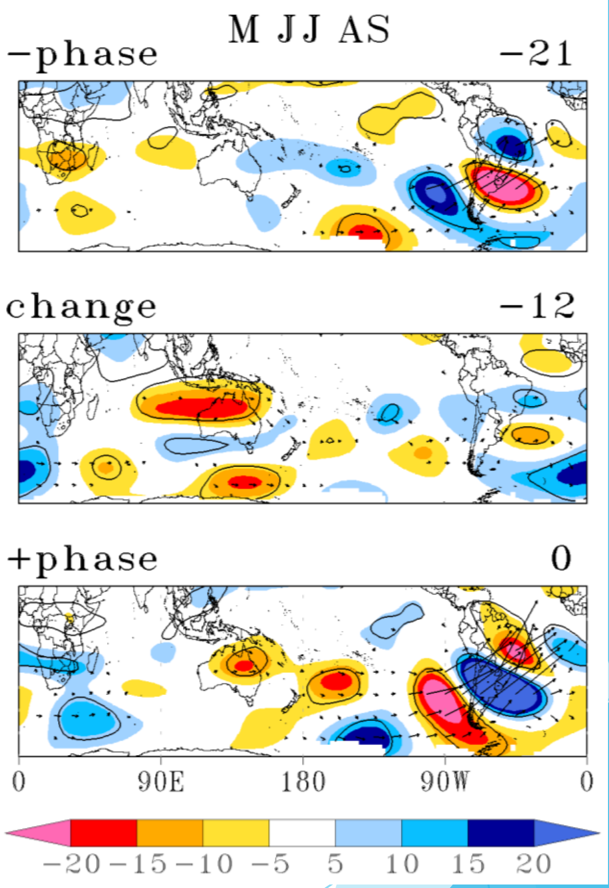

Maps of linear lagged regressions between OLR anomalies/ 0.21 sigma-level streamfunction and the standardized PC1 30-90 for MJJAS.

Rainy season: October to April | Dry season: March to September | IS variability in 30-90 days

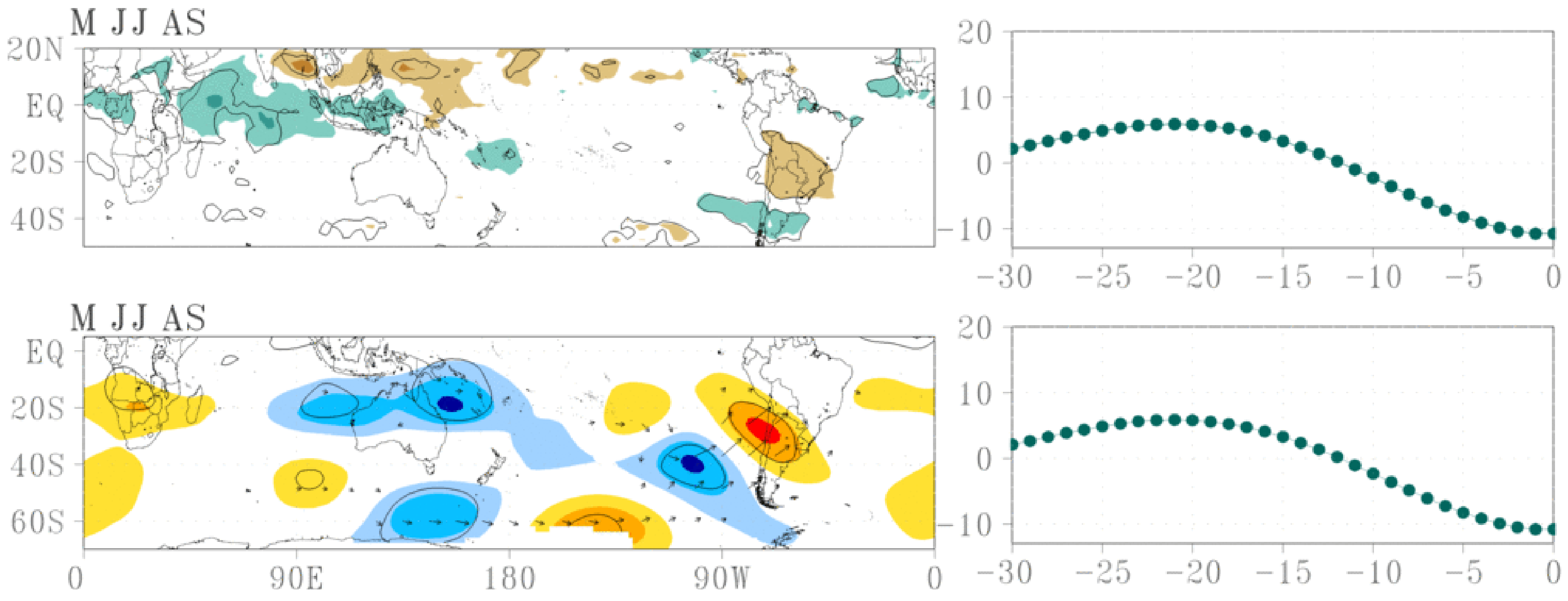

−30

Dry season: March to September | IS variability in 30-90 days

MJO index values for positive and negative SIS events

Positive SIS events

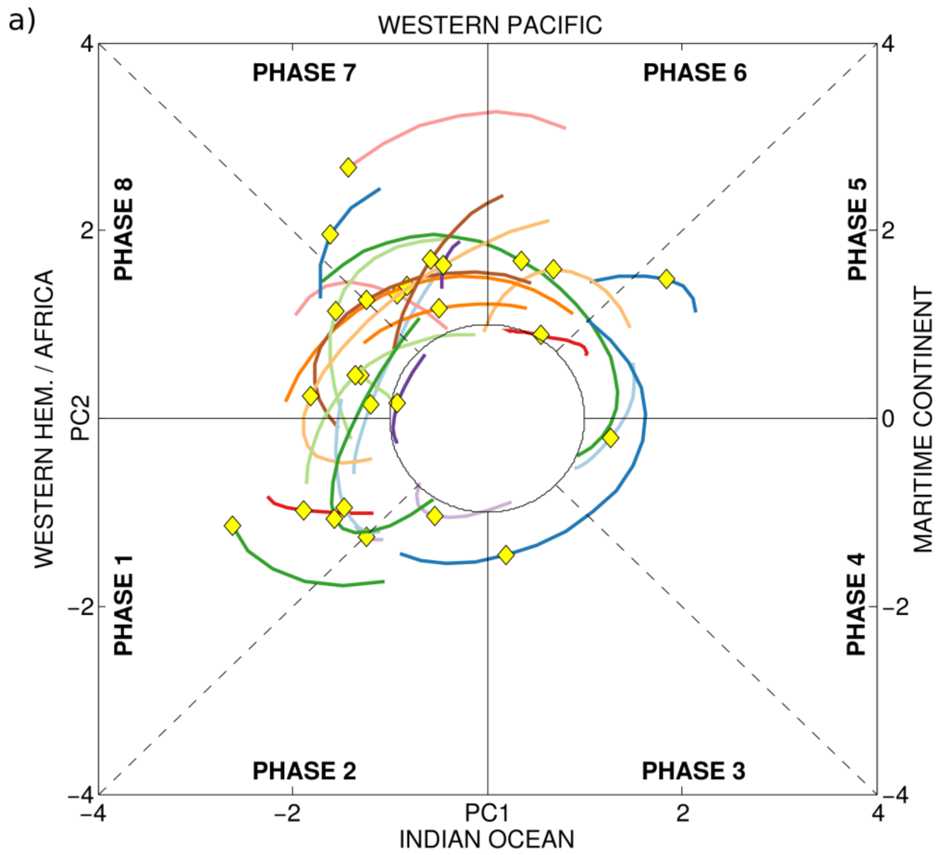

Negative SIS events

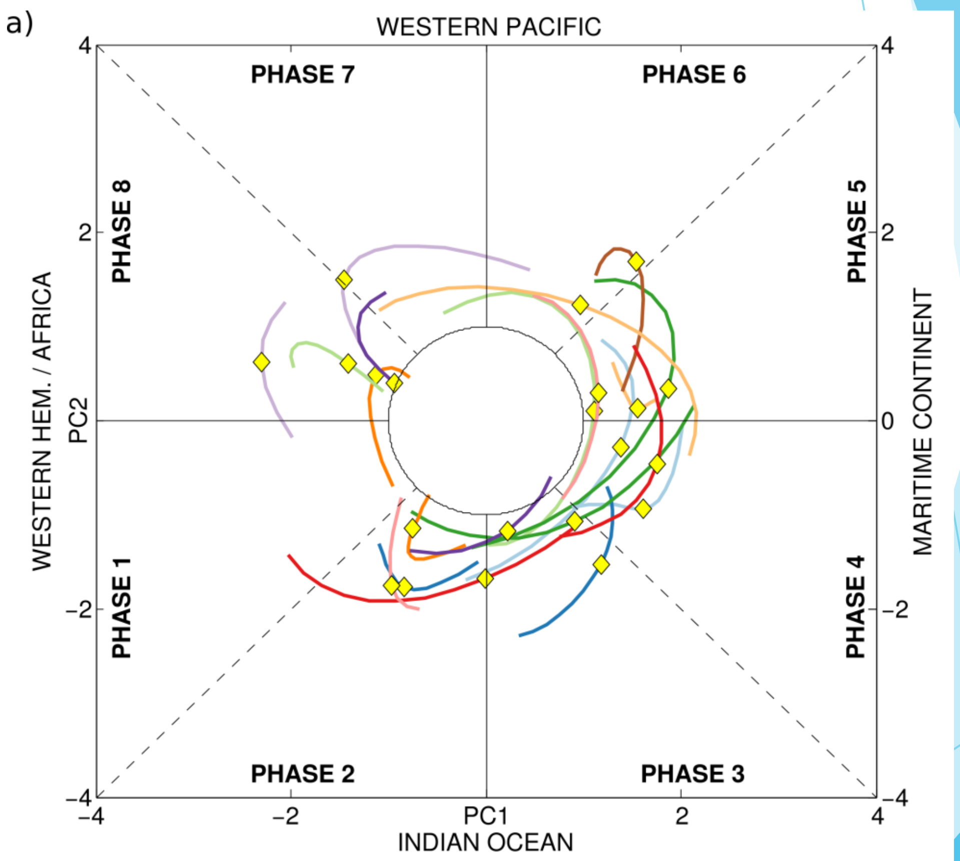

MJO phase diagram with the daily MJO index values during positive SIS events within an MJO event. The yellow diamond indicates the day in which the SIS index is maximum

Dry season: March to September | IS variability in 30-90 days

MJO index values for positive and negative SIS events

Positive SIS events

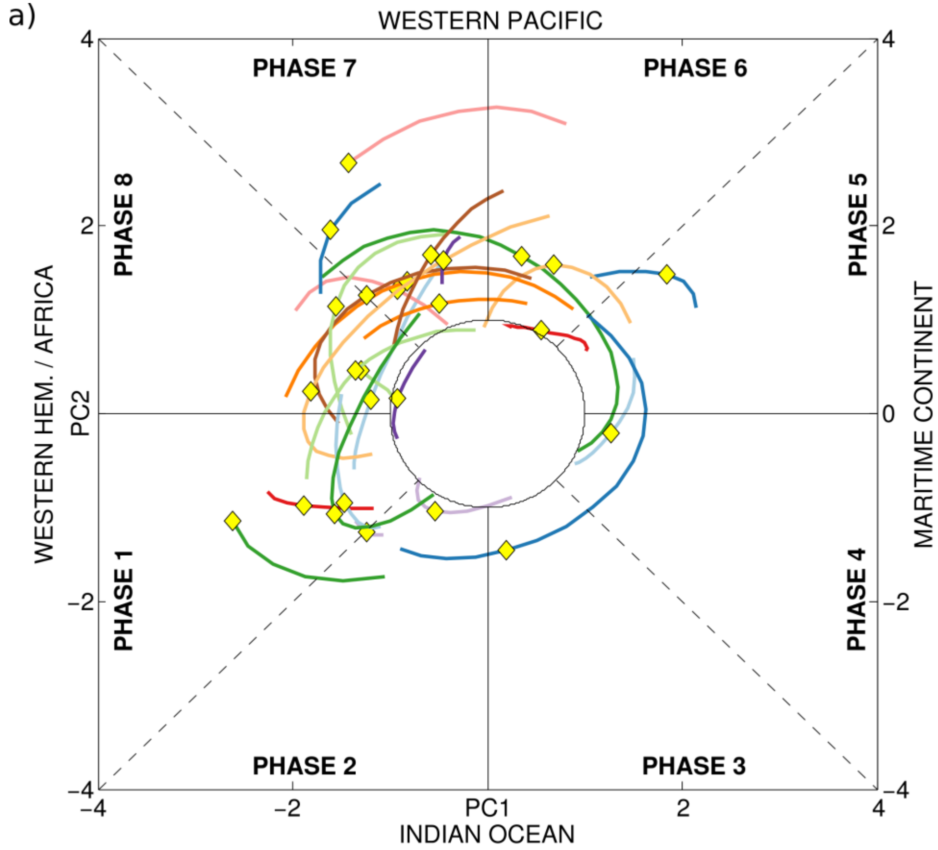

MJO phase diagram with the daily MJO index values during positive SIS events within an MJO event. The yellow diamond indicates the day in which the SIS index is maximum

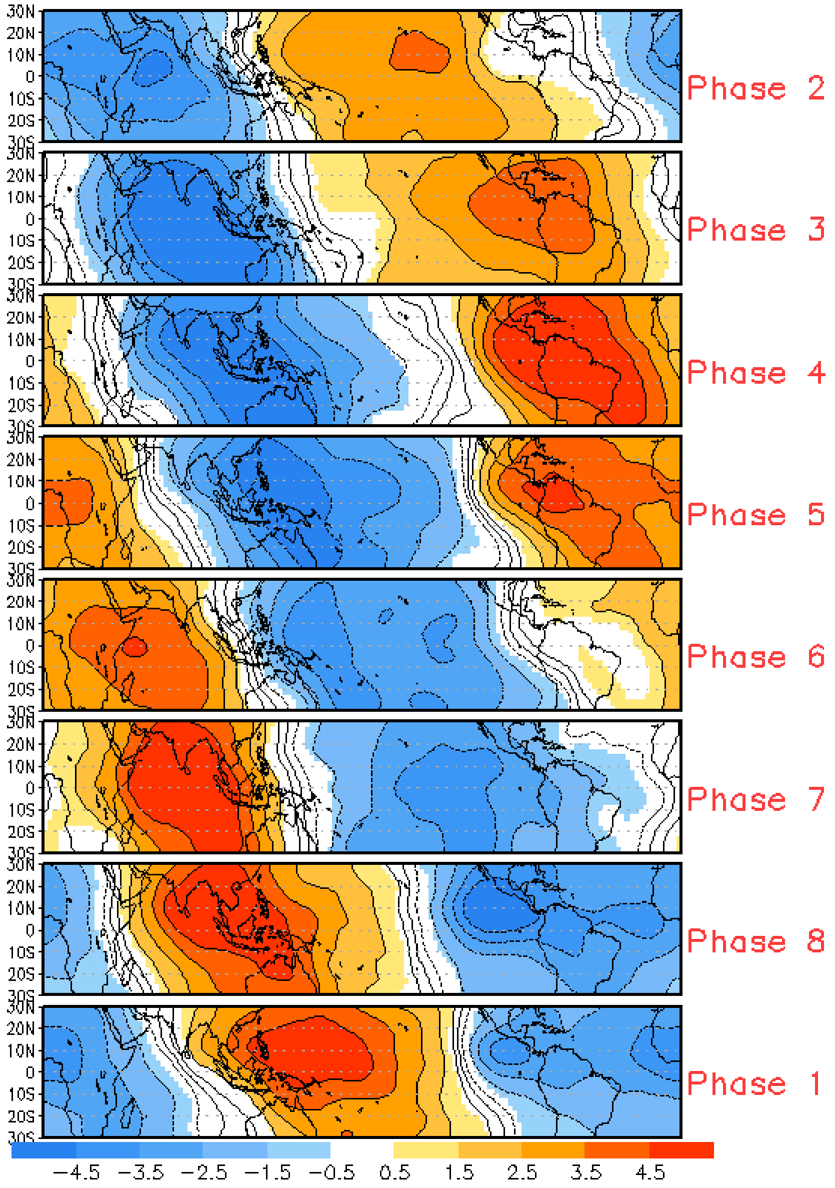

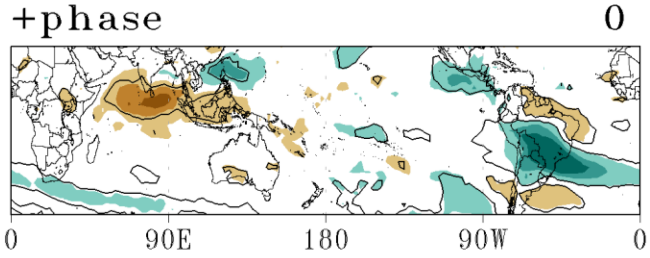

Dry season: March to September | IS variability in 30-90 days

Highlights

- During the **dry season**, the **SIS pattern** is a **monopole** extending over Paraguay and southeastern Brazil, with a NW-SE tilt. Explained variability of: 21.8%

- PC1-based lagged regressions showed that the evolution towards a positive phase of the SIS pattern is **not as clearly related to tropical convection** as it was during the rainy season. Also, alternating centers are observed upstream in the southwest Pacific. Extratropical wave trains are observed, along which energy is propagated. This resemble the PSA patterns.

- The relation between **SIS events and MJO events is not as clear as during the rainy season**. Still, it could be seen that SIS positive events might be favored when MJO phases are 6,7,8,1, while negative SIS events might be during MJO phases 2,3,4,5.

To address

- Disentangle the MJO signal on SIS events to analyze the phase in which the teleconnections that impact in SESA are first generated (precursors of SIS events).

- Use OMI to characterize MJO events and compare to these results.

All year | IS variability in 10-30 days

1030-SIS Pattern

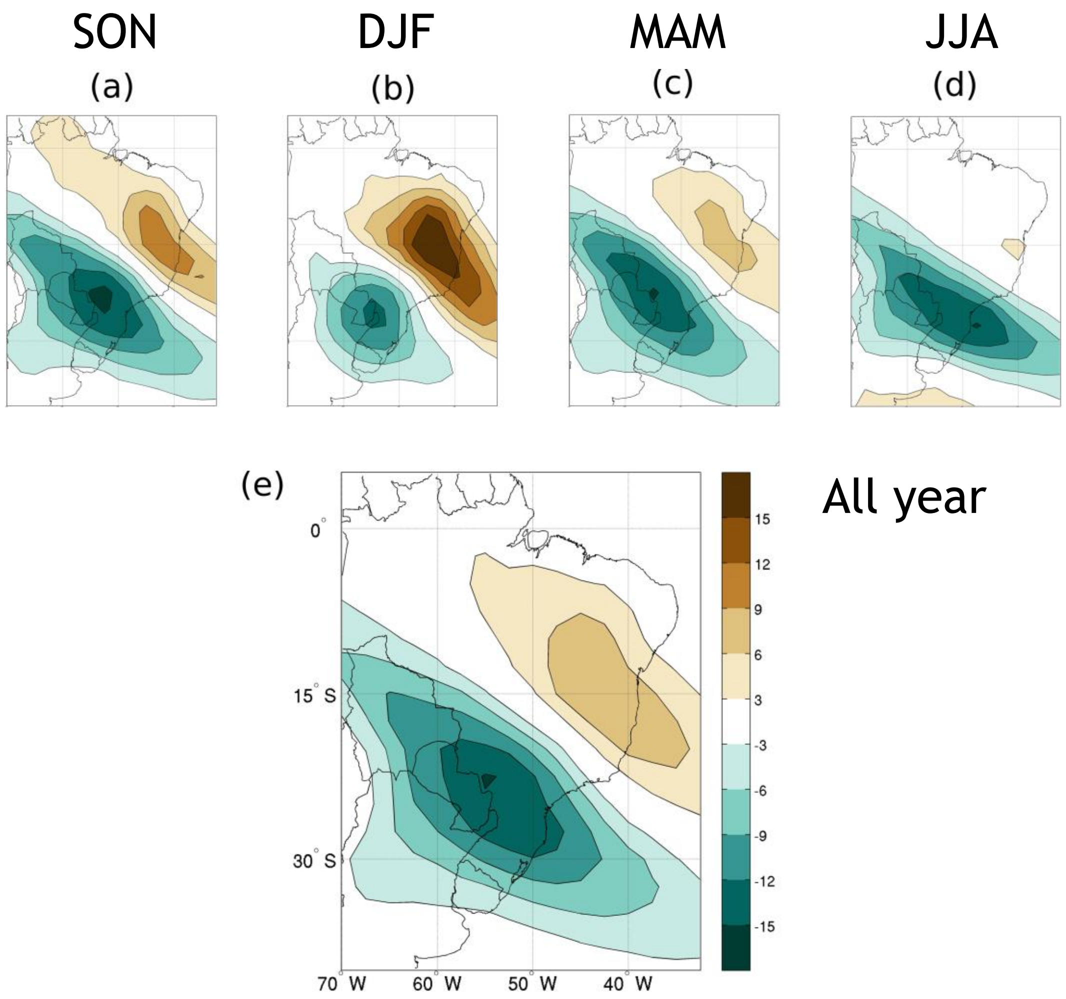

First EOF of FOLR 10-30 (15,3% of explained variance)

In the short IS time scale (10-30 days) it was found that even though there are seasonal differences in the SIS patterns along the year, it is still possible to represent **with only one SIS pattern** the variability associated to its evolution.

Using only one pattern is convenient not only for the sake of simplicity, but for making easier the tasks of real-time monitoring and prediction of the patterns.

All year | IS variability in 10-30 days

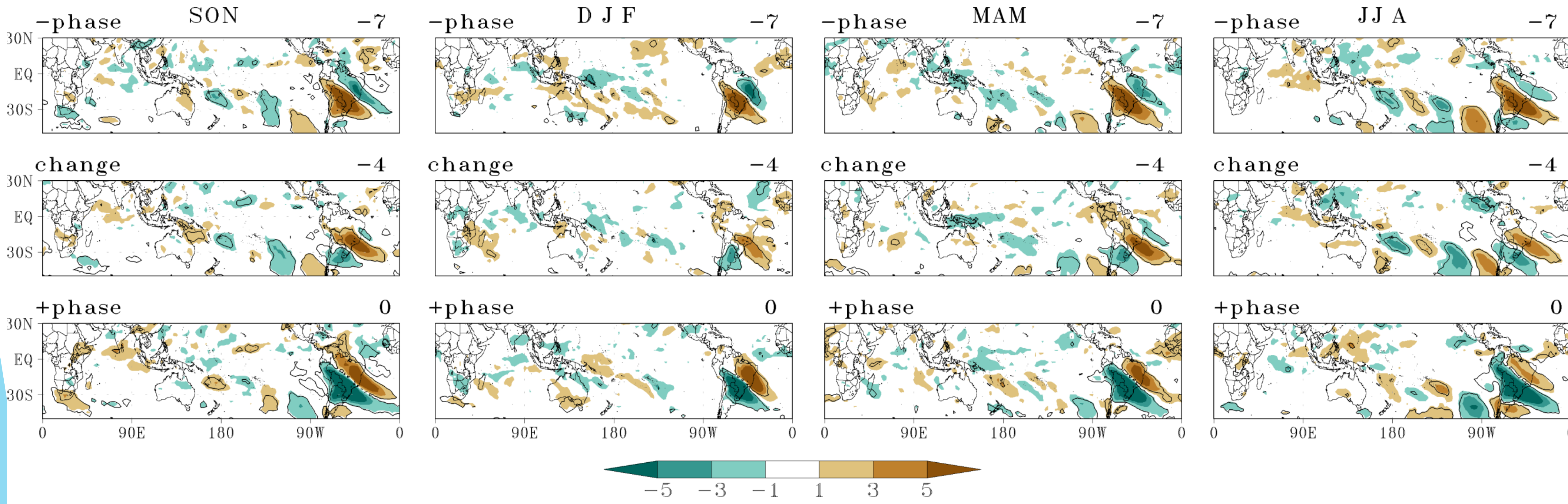

Maps of linear lagged regressions between OLR anomalies and the standardized PC1 10-30 for each season, for those lags in which the leading pattern of FOLR 10-30 showed the most intense negative phase, a change of phase and the most intense positive phase

All year | IS variability in 10-30 days

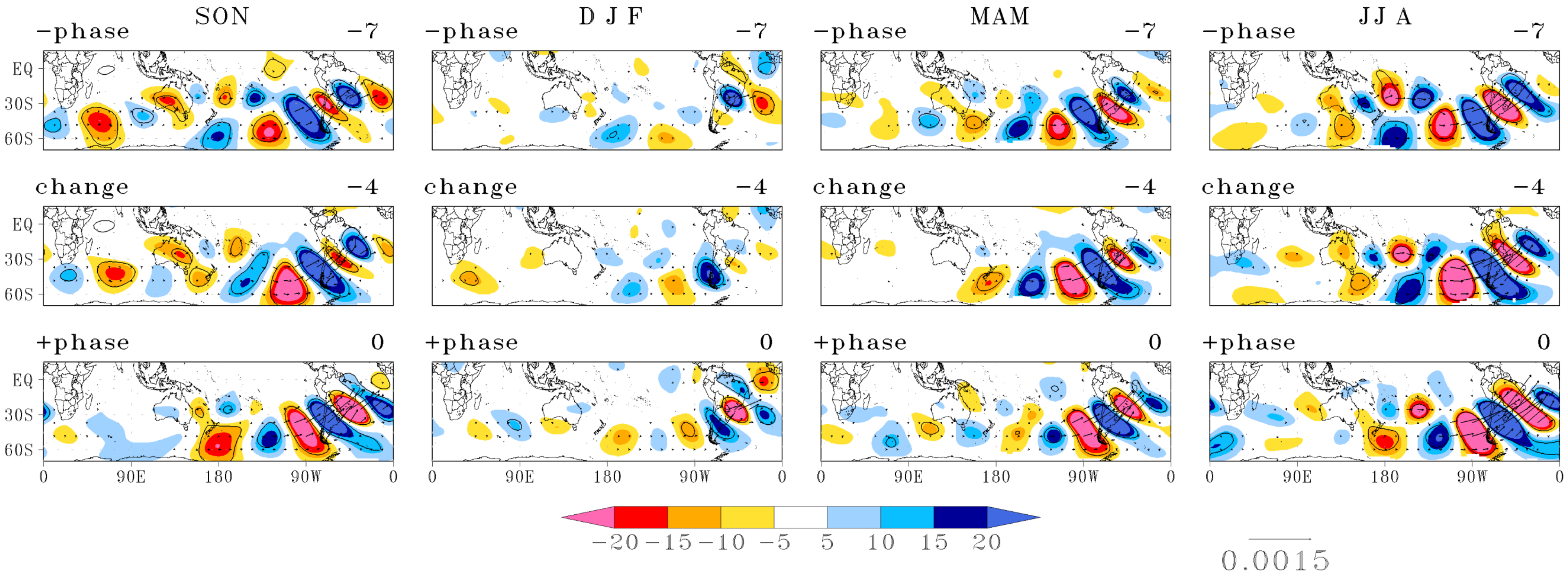

Maps of linear lagged regressions between 0.21 sigma-level streamfunction anomalies and the standardized PC1 10-30 for each season, for those lags in which the leading pattern of FOLR 10-30 showed the most intense negative phase, a change of phase and the most intense positive phase

All year | IS variability in 10-30 days

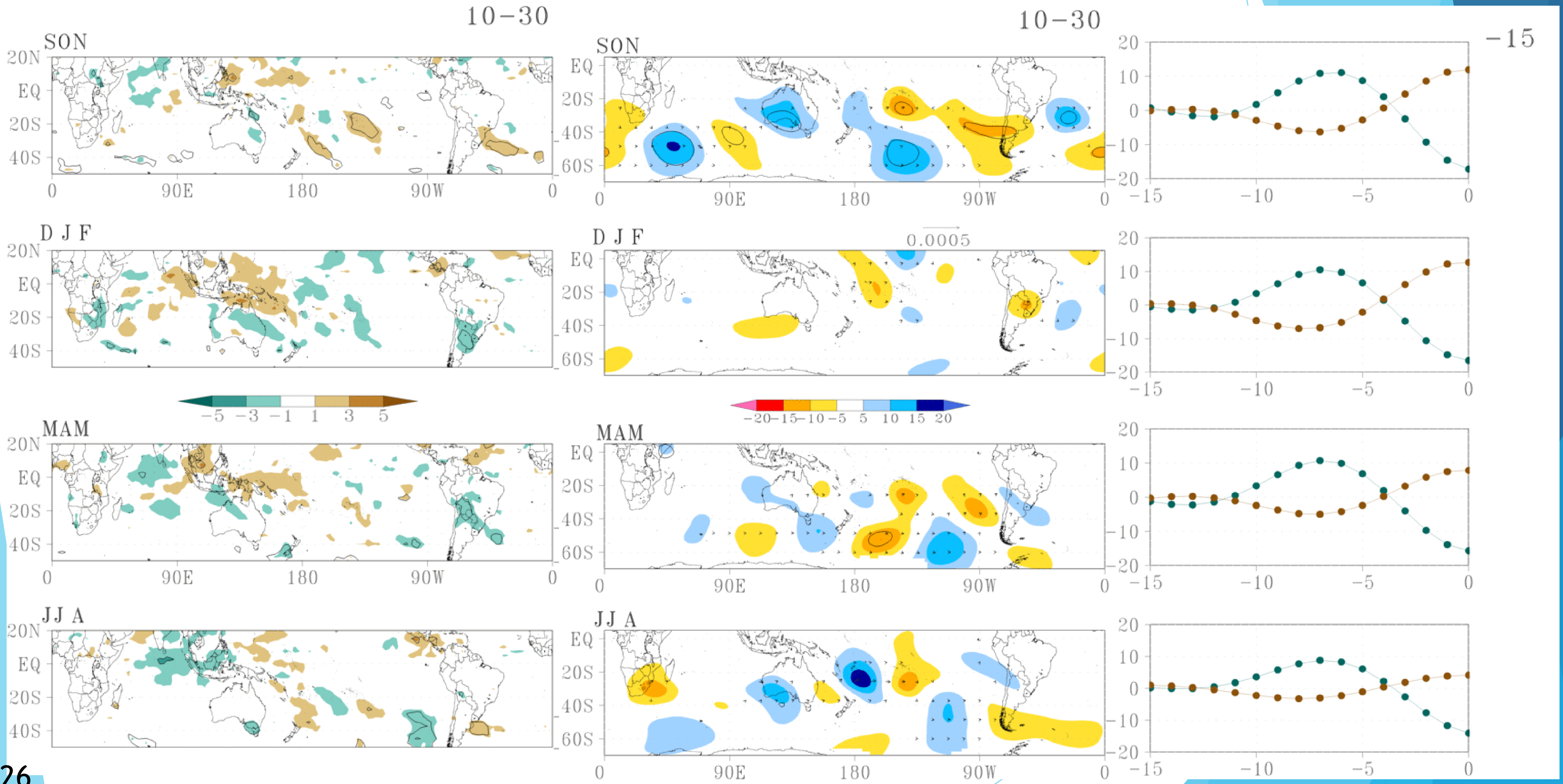

All year | IS variability in 10-30 days

Highlights

- The IS variability in the 10-30-day time scale can be described across all year using only one EOF, which explains 15.5% of the variance.

- The evolution of **convective anomalies do not show a propagation along tropical latitudes**, as expected. The influence of the SPCZ on the wave trains might not be observed with this linear approach. Raupp et al. (2008, 2010) showed that the nonlinear processes of resonance of equatorial waves lead to internal IS variability, and associated this process with tropical convection.

- The leading regional pattern is associated with the evolution of circulation anomalies organized in **strong, arched subpolar wave trains over the South Pacific Ocean**. The associated wave energy dispersion maintains a strong circulation anomaly with NW-SE-tilt over subtropical South America, being cyclonic in association with enhanced convection in SESA.

- During **JJA** and **SON**, a **strong subtropical wave** train is also detected, being absent during DJF.

To address

- Advance in the understanding of the IS variability in the 10-30-day band. How do nonlinear processes influence the region? Origin of the forcing? Case studies to avoid smoothing?

Current efforts on developing monitoring and forecast tools using the SIS pattern: climar.cima.fcen.uba.ar